American Mineralogist, Volume 78, pages 405–414, 1993

Formation of protective surface layers during silicate-mineral weathering under well-leached, oxidizing conditions

MICHAEL ANTHONY VELBEL
Department of Geological Sciences, 206 Natural Science Building, Michigan State University, East Lansing, Michigan 48824, U.S.A.

ABSTRACT

Formation of a protective surface layer [a layer of products through which transport (diffusion) of aqueous reactants or products is rate-determining] during silicate-mineral weathering requires that (1) elements normally considered immobile (e.g., Al, Fe) behave conservatively; and (2) the volume ratio of product to reactant be greater than one. Mineral suites involving most major rock-forming silicates (feldspars, pyroxenes, amphiboles, and olivines) weathering to common oxides and 1:1 clays are characterized by $V_{prod} < V_{react}$ ($V_{prod}/V_{react} < 1$). Protective surface layers cannot form on these minerals; instead, etch pits and porous pseudomorphs formed by interface-controlled reactions are ubiquitous. However, reactant-product mineral suites involving almandine and spessartine garnets are characterized by $V_{prod} > V_{react}$ ($V_{prod}/V_{react} > 1$). Weathered almandine and spessartine commonly exhibit laterally continuous, nonporous surface layers underlain by smooth, rounded reactant-mineral surfaces. The rate-determining step during weathering in these instances is diffusion through the surface layer of weathering products. Elemental mobility in the weathering environment and product-reactant volume ratios determine the occurrence of surface features (etch pits vs. protective surface layers) and associated rate-determining mechanisms (interface- vs. transport-controlled kinetics).

INTRODUCTION

The purpose of this paper is to propose a hypothesis: The presence or absence of protective surface layers during natural weathering of silicate minerals and the rate-determining mechanism of the weathering reactions are determined by the stoichiometries and molar volumes of reactant minerals and their weathering products. To test the molar volume hypothesis, product-reactant volume ratios are calculated for a number of common rock-forming silicate minerals, weathering to well-crystallized secondary minerals typical of thoroughly leached, oxidizing weathering conditions. Volume ratios are then related to the observed distribution of etch pits and surface layers on naturally weathered silicate minerals. Fe-bearing silicates are emphasized because of the equivocal nature of previous results regarding rate-determining mechanisms and protective surface layers on these minerals. The reactant and product minerals investigated here are listed in Table 1.

Rate-determining mechanisms in the weathering of major Fe-free rock-forming silicates

Any mineral-H_2O reaction (for example, hydrolysis of silicate minerals during rock weathering) requires a sequence of steps for the reaction to proceed. With the assumption that all reactants are available in excess, the following steps must occur (in order): (1) aqueous reactants (e.g., H ions or hydronium) must arrive at the mineral-solution interface, (2) the reaction must occur at the interface, and (3) dissolved products (e.g., alkali or alkaline earth cations, aqueous silica) must leave the site of the interfacial reaction (lest they accumulate to the extent that equilibrium is attained or the reaction is otherwise suppressed).

When a number of different reaction steps occur in series, the slowest step is rate determining. Therefore, one of two mechanisms is rate determining in the weathering of silicate minerals: (1) transport control (or transport-limited reaction), in which transport of aqueous reactants to or products from the fresh mineral surface is the slow step in the reaction; or (2) surface-reaction (interface) control (or interface-limited reaction), in which the rate of reaction is determined by processes occurring at the mineral-solution interface (Berner, 1978, 1981). Each rate-determining mechanism has unique consequences for the microscopic surface morphology of weathered mineral grains (Berner, 1978, 1981).

Surfaces of minerals dissolving by transport control are smooth, rounded, and featureless, reflecting the uniformity of attack on the surface (Berner, 1978, 1981). Diffusion is the slowest form of transport (Berner, 1978, 1981); the medium through which diffusion occurs may be the surrounding fluid, or a protective surface layer of residual or secondary solids on the surface of the dissolving mineral (armoring precipitate, as used by Schott and Petit, 1987; a surface layer is protective if diffusion of reactants or products through it is the rate-determining

0003–004X/93/0304–0405$02.00

step in the alteration reaction). However, measured silicate-mineral dissolution rates are too slow to be accounted for by aqueous diffusion (Berner, 1978, 1981), and no direct evidence of appreciable stoichiometrically altered surface layers has been reported from naturally weathered Fe-free major rock-forming silicates. Direct examination of the surfaces of many naturally weathered silicates instead reveals ubiquitous etch pits (crystallographically controlled dissolution voids; see reviews by Velbel, 1986, 1987; Blum and Lasaga, 1987; Schott and Petit, 1987). Etch pits and related features are produced by interface-limited mechanisms, reflecting the site-selective nature of the interfacial process (Berner, 1978, 1981; Brantley et al., 1986; Lasaga and Blum, 1986; Schott and Petit, 1987; Blum and Lasaga, 1987; Blum et al., 1990; Gratz et al., 1991a, 1991b). Clay pseudomorphs after aluminosilicates possess abundant porosity between clay crystallites in the pseudomorph (e.g., Glasmann, 1982; Velbel, 1983; Nahon and Bocquier, 1983; Anand and Gilkes, 1984). Diffusion through this open pore network is not likely to be sufficiently slow to affect reaction rates at the solid-fluid interface (e.g., Petrovic, 1976). Interface control is now favored for weathering of major rock-forming silicates, including (1) quartz, (2) feldspars, (3) Fe-free pyroxenes, amphiboles, and olivines, and (4) Fe-bearing pyroxenes, amphiboles, and olivines under reducing or extremely acidic conditions (e.g., Wilson, 1975; Berner and Holdren, 1977, 1979; Berner et al., 1980; Schott et al., 1981; Velbel, 1984b, 1986, 1987, 1989; Schott and Petit, 1987; Blum et al., 1990; Gratz et al., 1991a, 1991b).

TABLE 1. Stoichiometric coefficients and molar volumes for rock-forming silicate minerals and some weathering products characteristic of well-leached environments

Mineral	Element (*e*)	n_e	V^0
Common rock-forming aluminum and iron silicates			
Anorthite	Al	2	100.610
Low albite	Al	1	100.054
Orthoclase	Al	1	108.283
Ferrosilite	Fe	2	65.941
Anthophyllite	Fe	1.47	265.88
Cummingtonite	Fe	2.3	271.68
Fayalite	Fe	2	46.290
Other rock-forming silicates			
Almandine	Al	2	115.43
	Fe	3	
Spessartine	Al	2	117.88
	Mn	3	
Staurolite	Fe	4	445.67
	Al	18	
Zoisite	Al	3	136.19
Epidote-1	Al	2.16	138.146
	Fe	0.84	
Epidote-2	Al	2.60	137.370
	Fe	0.40	
Oxide			
Magnetite	Fe	3	44.528
Weathering products			
Kaolinite	Al	2	99.236
Gibbsite	Al	1	32.222
Goethite	Fe	1	20.693
Hematite	Fe	2	30.388
Lepidocrocite	Fe	1	22.492
Boehmite	Al	1	19.507
Diaspore	Al	1	17.862
Bayerite	Al	1	31.15
Nordstrandite	Al	1	32.28
Pyrolusite	Mn	1	16.708
Ramsdellite	Mn	1	17.838

Note: Stoichiometries and molar volumes for Tables 1–3 are from Smyth and Bish (1988) for all minerals except bayerite and nordstrandite (from Maynard, 1983) and lepidocrocite (calculated from unit-cell parameters given by Schwertmann and Taylor, 1989).

Ferromagnesian-silicate weathering

The evidence for weathering mechanisms of Fe-bearing pyroxenes, amphiboles, and olivines under oxidizing conditions is equivocal (Velbel, 1987). Although hydrous ferric oxide precipitates form during weathering of these minerals (Siever and Woodford, 1979; Berner and Schott, 1982; Schott and Berner, 1983, 1985; White et al., 1985; White and Yee, 1985) their potential diffusion-limiting role is still not well understood. The ubiquitous occurrence of etch pits and related features (Fig. 1) on soil pyroxenes, amphiboles, and olivines favors interface-controlled mechanisms (Berner and Schott, 1982; Velbel, 1987). Figure 1 is a scanning electron microscope (SEM) image of a denticulated margin (also known as cockscomb termination and hacksaw termination) on a naturally weathered inosilicate (hornblende), in which the teeth parallel the **c** axis of the reactant chain silicate (e.g., Berner et al., 1980; Berner and Schott, 1982; Velbel, 1987, 1989, and references therein; this feature is also common on weathered pyroxenes). This feature is also visible by optical petrography (e.g., Cleaves, 1974; Delvigne, 1983, 1990; Velbel, 1987, 1989). Berner et al. (1980) showed that etch features reflect selective attack at crystal defects and dislocations; the sharp denticulations result from side-by-side coalescence of lenticular (almond-shaped) etch pits (Berner et al., 1980; Berner and Schott, 1982). Etch pits (Fig. 2) and denticulated margins form on weathered olivines in the same manner (Wilson, 1975; Grandstaff, 1978; Delvigne et al., 1979; Nahon et al., 1982; Macaire et al., 1988). Mobilization of Fe by reduction in wet, O-depleted soils or exceptionally acidic settings accounts for only a few of the many natural occurrences of etched pyroxenes and amphiboles (Glasmann, 1982; Anand and Gilkes, 1984).

Boxworks (typically ferruginous) comprise a rigid network of secondary products that pseudomorphically preserves pyroxene and amphibole grain outlines and cleavages (with abundant porosity within the boxwork) even upon complete removal of the reactant-mineral remnants (e.g., Cleaves, 1974; Velbel, 1989; Delvigne, 1983, 1990). Densely etched or denticulated mineral surfaces are ubiquitous on most naturally weathered major rock-forming silicates, even on surfaces beneath clay coatings or oxide and hydroxide products (e.g., boxworks), from which the mineral surface is commonly separated by void (e.g., Cleaves, 1974; Nahon and Bocquier, 1983; Velbel, 1989; Delvigne, 1990; Nahon, 1991). This suggests that all portions of the primary mineral surface are accessible to fluids in spite of the precipitates.

Fig. 1. Denticulated margin on naturally weathered hornblende, formed by side-by-side coalescence of lenticular (almond-shaped) etch pits. Sample is from a weathered corestone developed on the Carroll Knob Complex, in the Blue Ridge near Otto, North Carolina (Velbel, 1989). Scanning electron photomicrograph; scale bar is 10 μm long.

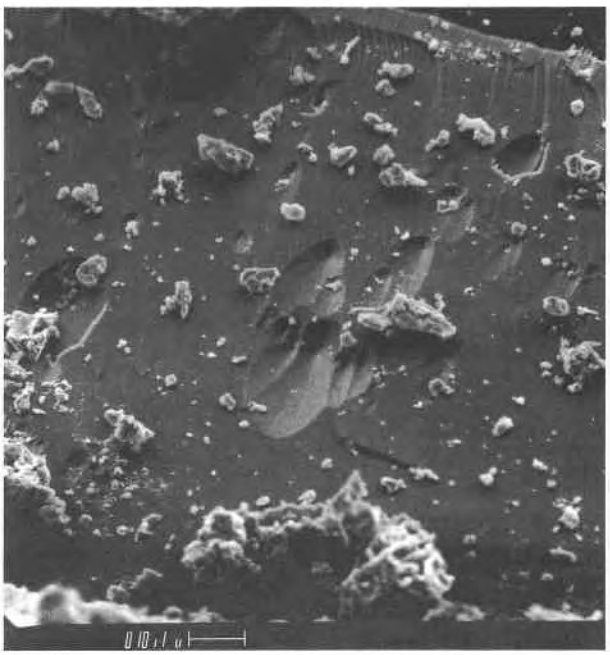

Fig. 2. Etch pits on naturally weathered olivine from a slightly weathered corestone in spheroidally weathered basalt near Schofield Barracks, Oahu, Hawaii. Note both individual etch pits and spatial arrays of overlapping pits. In order to minimize preparation artifacts (Cremeens et al., 1987), no chemical or mechanical pretreatment was employed; the dust adhering to the surface consists of natural fines produced and redistributed during sample shipping and storage. Scanning electron photomicrograph; scale bar is 10 μm long.

Garnet weathering

Studies of naturally weathered almandine garnet by Stoops et al. (1979), Parisot et al. (1983), Embrechts and Stoops (1982), and Velbel (1984a) provide considerable evidence that almandine weathers by a transport-controlled (diffusion-limited) mechanism in oxidizing weathering environments such as saprolite (Velbel, 1984a). In many soils, almandine surfaces are directly exposed to soil solutions (Velbel, 1984a; Ghabru et al., 1989; Graham et al., 1989a). These grains exhibit numerous well-formed etch pits (Fig. 3), indicating interface-control of garnet weathering in these weathering environments (Velbel, 1984a). However, in many lateritic and saprolitic regoliths, layers of limonite replace garnet. The replacement begins at grain boundaries and internal fractures traversing the garnet, and the replacement front evolves from the original grain boundary toward the grain or fragment center, a texture known as centripetal replacement (Parisot et al., 1983; Velbel, 1984a). The resulting products occur as layers of uniform thickness (Stoops et al., 1979; Embrechts and Stoops, 1982; Parisot et al., 1983; Velbel, 1984a). In thin section, the contact between the garnet surface and the layer of weathering products is sharp and smooth, and garnet subgrain corners (e.g., at the junctions of fractures) are commonly visibly rounded beneath the layers.

Scanning electron microscope (Fig. 4) and X-ray diffraction (XRD) observations show that the limonite consists of radially oriented fibrous intergrowths of gibbsite and goethite that formed by centripetal replacement of garnet (Velbel, 1984a; Graham et al., 1989b, report hematite as the ferruginous product in their material). Etch pits are absent. Diffusion (transport) of reactants and products through the gibbsite-goethite layer is the rate-determining step in the weathering of almandine in the oxidizing environment of the saprolite (Velbel, 1984a). Both coated and uncoated almandine grains can occur in the same soil (Graham et al., 1989a); garnets that were partially weathered in saprolites have thick coatings of limonite and persist in soils, whereas garnets that bypassed the coating-forming, saprolitic stage of weathering (i.e., were removed to soils directly from fresh outcrops) weather much more readily (Embrechts and Stoops, 1982). These observations further attest to the protective nature of the coatings. Similar features on manganiferous garnets (Nahon et al., 1984, 1985; Perseil and Grandin, 1985) suggest that similar weathering mechanisms prevail in these instances as well. These findings are significant because they include the first direct evidence that a protective surface layer exists on any naturally weathered silicate mineral (Velbel, 1984a, 1987).

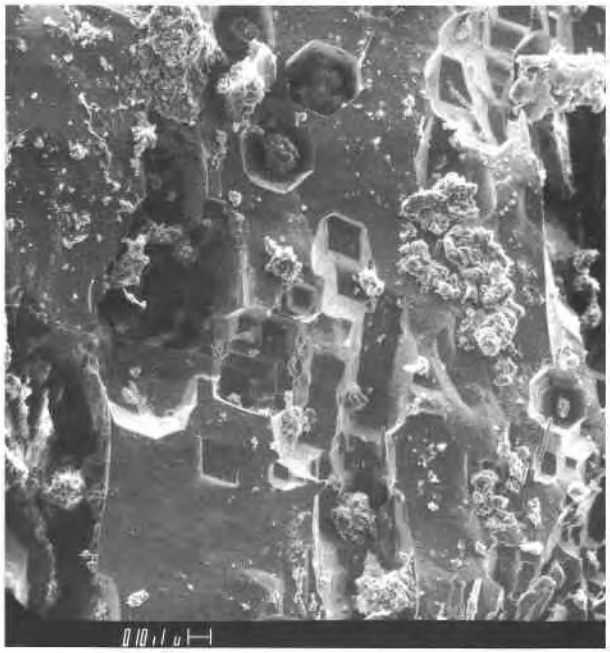

Fig. 3. Etch pits on naturally weathered almandine garnet. Sample is from shallow horizons of soil developed on the Precambrian Coweeta Group, in the Blue Ridge near Otto, North Carolina (Velbel, 1984a). Scanning electron photomicrograph; scale bar is 10 μm long.

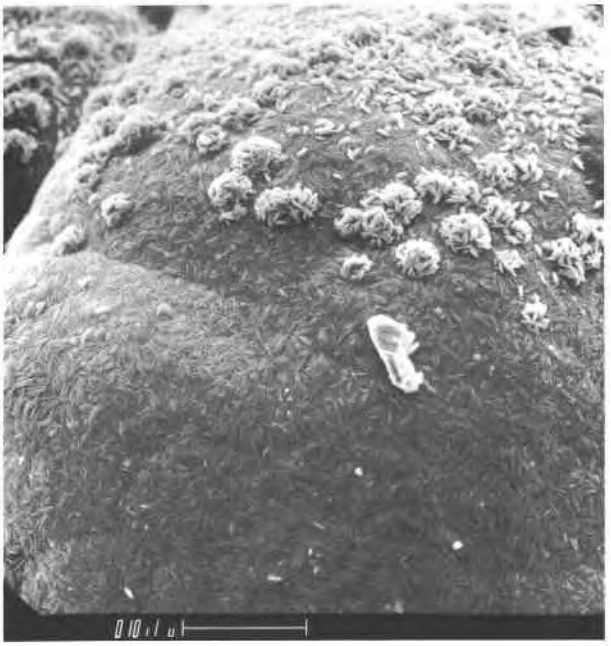

Fig. 4. Outer surface of limonite (gibbsite and goethite) surface layer formed by centripetal replacement during weathering of almandine garnet. Cross-sectional views through surface layer show that it consists of radially oriented gibbsite and goethite and provide additional evidence of centripetal replacement (Velbel, 1984a). Note the absence of shrinkage cracks or other voids, despite desiccation during sample storage and preparation for SEM. Sample is from deep weathering profile (saprolite) developed on Precambrian Tallulah Falls Formation in the Blue Ridge near Otto, North Carolina (Velbel, 1984a). Scanning electron photomicrograph; scale bar is 10 μm long.

Unanswered questions

1. It is now generally accepted that a protective surface layer does not form on naturally weathered pyroxenes and amphiboles (Berner and Schott, 1982; Velbel, 1987). Does a nonprotective surface layer of secondary minerals form on weathered ferromagnesian silicates, which is too thin, too porous, or otherwise unable to be transport limiting, but still compositionally altered (Berner and Schott, 1982)?

2. Why do thick protective surface layers not form on naturally weathered pyroxenes, amphiboles, or olivines (Berner and Schott, 1982; Velbel, 1984b, 1987, 1989), whereas such layers do appear to form on Fe- and Mn-bearing garnets (at least under certain conditions; Stoops et al., 1979; Embrechts and Stoops, 1982; Parisot et al., 1983; Velbel, 1984a, 1987; Nahon et al., 1984, 1985; Perseil and Grandin, 1985)?

3. What combination of mineralogical factors of the primary mineral (e.g., structure or major-element composition) and geochemical (e.g., redox, leaching, acidity) conditions in the weathering environment determine the circumstances under which a potentially protective surface layer can form during silicate-mineral weathering?

Methods

The approach used here is analogous to the Pilling-Bedworth rule, widely used by metallurgists to explain and predict the corrosion of metals (e.g., Kubaschewski and Hopkins, 1962; Hauffe, 1965). The Pilling-Bedworth criterion states that thick oxide layers that form on reactant metal during oxidation are adherent and pore free (i.e., protective, in that diffusion through them is rate determining) if V_p/V_r (where V_p is the volume of product and V_r is the volume of reactant) > 1 (Kubaschewski and Hopkins, 1962; Hauffe, 1965). By analogy with the Pilling-Bedworth rule, the potential for any primary rock-forming silicate mineral to form a protective surface layer during weathering may be estimated by calculating the volume of secondary minerals that would form from a given volume of reactant, if one assumes conservative behavior of the least mobile elements. A protective surface layer can form only if geochemical conditions permit conservative behavior of elements like Al, Fe, or Mn, and if $V_p/V_r \geq 1$. If product-forming elements behave nonconservatively (e.g., because of chelates enhancing the solubility of otherwise immobile elements such as Al, or weathering under reducing conditions, mobilizing Fe or Mn), or if $V_p/V_r < 1$, formation of a sufficient volume of products to result in a continuous, uninterrupted layer of products capable of occluding primary-mineral surface area is impossible, and the surface is vulnerable to direct attack, with interface-limited kinetics. Etched, product-poor surfaces result.

The Pilling-Bedworth rule appears to be important for reaction products in which diffusion of matter is from the outer surface of the product toward the metal-product interface (Kubaschewski and Hopkins, 1962; also, Fromhold, 1976), a geometry precisely analogous to the observed centripetal garnet replacement textures (e.g., Velbel, 1984a, 1987). Reactant-product molar volumes have also been used in investigations of rate-determining mechanisms of weathering, hydrothermal alteration, and pseudomorphous replacement of Ti minerals that are natural analogues for ceramic high-level radioactive wasteforms (Hollabaugh et al., 1989; Vance and Doern, 1989).

The total number of moles of a given element (e) in any arbitrary volume of reactant or product mineral is given by

$$m_{e,i} = \frac{n_{e,i} V_i}{V_i^0} \quad (1)$$

where $m_{e,i}$ = total number of moles of element e in mineral i, $n_{e,i}$ = stoichiometric coefficient of element e in mineral i, V_i = volume of mineral i, and, V_i^0 = molar volume of mineral i.

Writing two such equations (one for i = reactant mineral, r, and the other for i = product mineral, p), setting $m_{e,r} = m_{e,p}$ (that is, conserving element e, letting all of element e present in the reactant mineral be incorporated into the product mineral), combining the equations for reactant and product minerals, and rearranging, gives

$$\frac{V_p}{V_r} = \frac{n_{e,r} V_p^0}{n_{e,p} V_r^0} \quad (2)$$

where V_p/V_r is the volume of product mineral produced per unit volume of reactant mineral, if element e is conserved.

Molar volumes and stoichiometric coefficients for reactant and product minerals summarized in Table 1 are taken directly from the compilations of Smyth and Bish (1988) and Maynard (1983), or calculated from unit-cell parameters reported by Schwertmann and Taylor (1989).

Results

The calculated values of the product-reactant volume ratio for common rock-forming silicate minerals weathered under thoroughly leached oxidizing conditions are shown in Table 2. The maximum possible volume of aluminous secondary minerals that can be formed from common feldspars is from anorthite. Among ferromagnesian silicates, Fe end-members form the maximum possible volume of product. If Fe behaves conservatively, any real pyroxene, amphibole, or olivine with lesser Fe^{2+} components in solid solution will form a lesser volume of ferruginous product than the amount shown in Table 2.

Under well-leached, oxidizing conditions, no common rock-forming silicate mineral contains enough Fe or Al to form a thick, nonporous, protective surface layer of common secondary minerals (e.g., gibbsite, goethite, kaolinite, lepidocrocite) around itself. At best, a fraction of the original grain volume is occupied by weathering products. Void ratios (one minus the value shown in Table 2) for any individual reactant-product pair involving Fe− and Al− end-members of common rock-forming silicates range from 1.4 to 88.6 vol%. Void ratios are even higher if Al or Fe are mobilized. These void ratios are sufficient to render the products ineffective as barriers to transport of aqueous reactants or products (assuming the void space is interconnected).

Most other oxide and oxyhydroxide products of weathering, both common (hematite, boehmite, diaspore) and uncommon (bayerite) have molar volumes lower per Al or Fe than gibbsite or goethite (Table 1; Smyth and Bish, 1988; Maynard, 1983), so product-reactant volume ratios will be lower for these products and void ratios will be higher than the values indicated in Table 2 for goethite and gibbsite. These minerals are even less likely to form protective surface layers on common rock-forming silicates than are gibbsite and goethite. Even uncommon secondary minerals with larger molar volumes per Fe or Al (e.g., nordstrandite) cannot occur in sufficient volumes, if Al and Fe behave conservatively. The molar volume of nordstrandite is only 0.2% greater than that of gibbsite, and nordstrandite is rare as a weathering product (Maynard, 1983).

Feldspars, pyroxenes, amphiboles, and olivines cannot form protective surface layers of common weathering products under well-leached, oxidizing conditions (Table 2) and should all exhibit site-selective dissolution and etch pits under all circumstances (i.e., whether Fe and Al behave conservatively or not). This is consistent with the literature on natural weathering of these minerals, on which etch pits and related features are ubiquitous, and apparently protective coatings have never been reported (Wilson, 1975; Berner and Holdren, 1977, 1979; Berner et al., 1980; Berner and Schott, 1982; Velbel, 1984b, 1986, 1987, 1989).

Table 3 shows product-reactant volume ratios for some less common silicates. If Al, Fe, and Mn are conserved, certain combinations of weathering products [e.g., almandine → iron oxyhydroxide (goethite or lepidocrocite) + aluminum hydroxide (gibbsite or bayerite or nordstrandite)] have $V_p/V_r > 1$. These reactant-product combinations could form protective surface layers. Such apparently protective layers occur on some naturally weathered almandine (e.g., gibbsite + goethite, Fig. 4; Stoops et al., 1979; Embrechts and Stoops, 1982; Parisot et al., 1983; Velbel, 1984a, 1987) and spessartine (Nahon et al., 1984, 1985; Perseil and Grandin, 1985; Velbel, 1987).

Combinations of products that include aluminum oxyhydroxides (boehmite, diaspore) or iron oxides (hematite) form product assemblages with too little solid volume to form protective surface layers on garnets ($V_p/V_r < 1$; Table 3). Therefore, the factors that determine the specific secondary mineral formed in any particular weathering environment will also control, through the

TABLE 2. Reactant-product molar-volume relationships for common rock-forming silicate minerals

Reactant → product	Element conserved	V_{prod}/V_{react}
Anorthite → gibbsite	Al	0.640
Low albite → gibbsite	Al	0.322
Orthoclase → gibbsite	Al	0.298
Anorthite → kaolinite	Al	0.986
Low albite → kaolinite	Al	0.496
Orthoclase → kaolinite	Al	0.458
Ferrosilite → goethite	Fe	0.628
Anthophyllite → goethite	Fe	0.114
Cummingtonite → goethite	Fe	0.175
Fayalite → goethite	Fe	0.894
Ferrosilite → lepidocrocite	Fe	0.682
Anthophyllite → lepidocrocite	Fe	0.124
Cummingtonite → lepidocrocite	Fe	0.190
Fayalite → lepidocrocite	Fe	0.972

mineral relations of that product, the rate-determining mechanism of garnet weathering. However, drawing mechanistic inferences from product mineral relations alone (without information on textural relationships, for example, centripetal replacement textures) is hazardous. For instance, hematite is believed to form from almandine in at least some weathering profiles (Graham et al., 1989b). If almandine weathered directly to hematite, the calculations here suggest that the hematite-bearing product cannot have acted as a protective surface layer, even in combination with gibbsite (for products = gibbsite + hematite and reactant = almandine, $V_p/V_r = 0.953$; Table 3). However, if the hematite formed by dehydration of earlier formed goethite or lepidocrocite, the weathering product layer or pseudomorph will presently consist of

TABLE 3. Reactant-product molar-volume relationships for some less common rock-forming silicate minerals

Reactant → product	Element conserved	V_{prod}/V_{react}
Almandine → goethite	Fe	0.538
Almandine → gibbsite	Al	0.558
ALMANDINE → GOETHITE + GIBBSITE		1.096
Almandine → lepidocrocite	Fe	0.585
ALMANDINE → LEPIDOCROCITE + GIBBSITE		1.143
Almandine → bayerite	Al	0.540
ALMANDINE → GOETHITE + BAYERITE		1.078
ALMANDINE → LEPIDOCROCITE + BAYERITE		1.125
Almandine → nordstrandite	Al	0.559
ALMANDINE → GOETHITE + NORDSTRANDITE		1.097
ALMANDINE → LEPIDOCROCITE + NORDSTRANDITE		1.144
Almandine → hematite	Fe	0.395
Almandine → boehmite	Al	0.338
Almandine → diaspore	Al	0.310
Almandine → goethite + boehmite		0.876
Almandine → goethite + diaspore		0.848
Almandine → hematite + gibbsite		0.953
Almandine → lepidocrocite + boehmite		0.923
Almandine → lepidocrocite + diaspore		0.895
Spessartine → gibbsite	Al	0.547
Spessartine → pyrolusite	Mn	0.425
Spessartine → gibbsite + pyrolusite		0.972
Spessartine → ramsdellite	Mn	0.454
SPESSARTINE → GIBBSITE + RAMSDELLITE		1.001
Spessartine → kaolinite	Al	0.842
SPESSARTINE → KAOLINITE + PYROLUSITE		1.267
SPESSARTINE → KAOLINITE + RAMSDELLITE		1.296
Staurolite → goethite	Fe	0.186
STAUROLITE → GIBBSITE	Al	1.301
STAUROLITE → BAYERITE	Al	1.258
STAUROLITE → NORDSTRANDITE	Al	1.304
Staurolite → lepidocrocite	Fe	0.202
Staurolite → hematite	Fe	0.136
Staurolite → boehmite	Al	0.788
Staurolite → boehmite + lepidocrocite		0.990
Staurolite → boehmite + goethite		0.974
Staurolite → diaspore	Al	0.721
Zoisite → gibbsite	Al	0.710
ZOISITE → KAOLINITE	Al	1.09
Epidote-1 → gibbsite	Al	0.504
Epidote-1 → kaolinite	Al	0.776
Epidote-1 → goethite	Fe	0.126
Epidote-1 → kaolinite + goethite		0.902
Epidote-2 → gibbsite	Al	0.610
Epidote-2 → kaolinite	Al	0.939
Epidote-2 → goethite	Fe	0.060
Epidote-2 → kaolinite + goethite		0.999
MAGNETITE → HEMATITE (MARTITE)	Fe	1.02

Note: Capitalized entries are those reactant-product assemblages that exceed the Pilling-Bedworth criterion, favoring formation of protective surface layers and diffusion-limited reactions.

TABLE 4. Textural and kinetic consequences of elemental mobility and product-reactant molar-volume ratios

Immobile elements conserved?	No (removed)	Yes	Yes
Product-reactant volume ratio	Any value	$V_p/V_r < 1$	$V_p/V_r > 1$
Surface morphology of relict primary mineral grain	1. Bare grain surface 2. Etch pits	1. Product-poor grain surface 2. Etch pits	1. Protective surface layer 2. Smooth rounded reactant mineral surface
Rate-determining mechanism	Interface-limited	Interface-limited	Transport-limited
Examples (see text for references)	Feldspar, amphibole, pyroxene, olivine, garnet weathered in the presence of organic chelating agents (in soils) or under reducing conditions*	Feldspar, amphibole, pyroxene, olivine weathered in saprolite under oxidizing conditions	Almandine garnet and spessartine garnet weathered in saprolite under oxidizing conditions
Texture produced by complete destruction of primary mineral	Moldic dissolution void	Porous pseudomorph	Solid pseudomorph
Demonstrated or possible examples (references below)	Pyroxene, amphibole under Fe-mobile conditions*,**	Limonite or clay boxwork after pyroxene or amphibole†	Limonite or manganese oxide nodules after garnet‡

* Also, numerous examples of intrastratally dissolved detrital silicates (e.g., feldspars, heavy minerals) in sandstones.
** Glasmann, 1982; Anand and Gilkes, 1984.
† Basham, 1974; Cleaves, 1974; Delvigne, 1983, 1990; Velbel, 1989.
‡ Velbel, 1984a, 1987; Nahon et al., 1984, 1985; Perseil and Grandin, 1985.

hematite, but its precursor (goethite or lepidocrocite) may still have acted as a protective surface layer. Only textural evidence in samples that preserve remnant reactant garnet and its contact relationships with the product will reveal the pathway of hematite formation and the rate-determining role of the product in such instances. In the absence of information from replacement textures, the present mineral relations alone of a product assemblage with $V_p/V_r < 1$ are not sufficient criteria for dismissing the protective surface-layer hypothesis, or for confirming that the product itself was not rate determining.

Nonconservative behavior of potential coating-forming Al and Fe (Velbel, 1984a) causes etching of grain surfaces on some occurrences of naturally weathered almandine (e.g., Embrechts and Stoops, 1982; Velbel, 1984a, 1987; Graham et al., 1989a). If Al and Fe are removed by inorganic complex-forming anions or organic chelating agents in shallow soil solutions (or in the burial diagenetic environment; Hansley, 1987; Salvino and Velbel, 1989), by exceptional acidity in the weathering environment, or by reduction of Fe in wet, O-depleted soils, the protective surface layer cannot form, and site-selective, interface-limited attack on the garnet surface forms etch pits (Fig. 3; Velbel, 1984a, 1987). Intermediate cases are also possible; for example, limonite (gibbsite-goethite) septa sometimes preserve garnet grain boundaries and fractures but surround voids from which garnet has apparently been removed (Stoops et al., 1979; Embrechts and Stoops, 1982; Parisot et al., 1983; Velbel, 1984a, 1987). These might be due either to solid-solution effects or multistage weathering. If the actual garnet contains insufficient almandine or spessartine component (relative to the end-member values shown in Table 3) for the product/reactant ratio to exceed unity, then a porous pseudomorph forms, even if Al and Fe are conserved. Alternatively, if an early, Al- and Fe-conserving stage is followed by a stage in which Al and Fe are mobile, similar textures might result.

DISCUSSION

Three sets of mineralogical (product-reactant molar-volume ratios) and environmental conditions can be identified. Each set results in a specific rate-determining mechanism and associated suite of surface features on partially weathered relics of primary (reactant) mineral grains (Table 4).

1. Removal of Al, Fe, or Mn causes the formation of porous pseudomorphs (in the case of partial removal of the least mobile elements) or primary mineral surfaces completely devoid of any weathering products (in the case of complete removal), interface-controlled reaction kinetics, and etch pits. Any aluminosilicate or ferromagnesian silicate mineral (including almandine garnet and presumably other minerals like those listed in Table 3) can exhibit these features under conditions favoring removal of the key elements.

2. A chemical environment favoring Al, Fe, and Mn conservation, operating on a reactant-product mineral suite characterized by $V_p < V_r$ ($V_p/V_r < 1$) results in porous pseudomorphs, interface control, and etch pits.

The ubiquity of etch pits and interface-controlled reaction kinetics on naturally weathered feldspars, pyroxenes, amphiboles, and olivines (e.g., Figs. 1, 2), weathered to common oxides, oxyhydroxides, hydroxides, and 1:1 clays, can be explained by either of the above scenarios.

3. A reactant-product mineral suite characterized by $V_p > V_r$ ($V_p/V_r > 1$) weathering in a chemical environment favoring Al, Fe, or Mn conservation results in the formation of a protective surface layer with smooth, rounded surfaces on the reactant-mineral grain beneath the protective surface layer and transport-controlled kinetics. Of all the silicate minerals examined to date, only almandine and spessartine garnets have ratios greater than unity under normal leaching conditions, and then only for certain combinations of products. This scenario accounts for observed features of weathered almandine and spessartine

garnets (and probably staurolite and some epidote group minerals; see below).

The bulk volumetric calculations and presumed kinetic consequences presented here, although intended to relate to morphological features visible at petrographic and SEM scales, may also be correlated with smaller scale features. Reactant-product mineral suites characterized here by $V_p/V_r < 1$ include those (e.g., feldspar to clay) for which HRTEM studies suggest incoherent structural relationships between reactant minerals and their alteration products, and open, porous, amorphous intermediates between the reactant mineral and crystalline clay products (Eggleton and Buseck, 1980; Eggleton and Smith, 1983; Eggleton, 1986; Tazaki, 1986; Tazaki and Fyfe, 1987a, 1987b; Banfield and Eggleton, 1990). Such open fabrics would probably not inhibit transport of solutes to or from the fresh mineral surface (Eggleton and Buseck, 1980; Eggleton and Smith, 1983; Eggleton, 1986). Thus, the same compositional and structural (volumetric) attributes that influence product abundances, porosities, and transport properties at the micrometer scale may also be related to those same properties at the nanometer scale as well.

The same sets of conditions also relate to specific textural features resulting from complete alteration of the reactant mineral. These textures are also summarized in Table 4. Table 4 includes examples of textures from the lateritic, bauxitic, saprolitic profiles discussed here, as well as examples from burial diagenesis of sandstones.

The hypothesis that product-reactant molar volume ratios predict rate-determining mechanisms can be further tested. Under Al-conservative conditions (e.g., weathering in the vadose zone, below the soil zone where organic chelating agents might mobilize Al), naturally weathered staurolite should form a protective surface layer of aluminous hydroxide weathering products (gibbsite, bayerite, or nordstrandite) but not of aluminous oxyhydroxides (boehmite or diaspore), whether Fe behaves conservatively or not (Table 3). Zoisite can form protective surface layers of kaolinite, but layers consisting of aluminum hydroxides or aluminum oxyhydroxides will not be protective (Table 3). Although neither of the two specific epidote samples included in the compilation of Smyth and Bish (1988) contains sufficient Al + Fe to form protective surface layers, epidote even slightly more aluminous than those shown in Table 3 contains enough Al + Fe to form protective surface layers consisting of kaolinite ± goethite. Less aluminous epidote, or epidote weathering to gibbsite, cannot form protective surface layers. Studies of the weathering textures and mechanisms of these groups of minerals are in progress, to test the hypothesis presented here. The behavior of ferromagnesian silicate minerals in poorly leached alteration environments (e.g., those in which 2:1 phyllosilicates form as alteration products) will be the subject of a future contribution.

Summary

Volumetric relationships during weathering provide quantitative information on the distribution of major rate-determining mechanisms (transport-control by protective surface layers vs. site-selective interface-limited reactions that produce etch pits) among major mineral groups, under various conditions of conservative or nonconservative behavior of key elements. The product-reactant volume ratio is always less than unity for common rock-forming silicates (feldspars, pyroxenes, amphiboles, and olivines) weathered under thoroughly leached, oxidizing conditions, even for Fe- and Al-rich end-members. This explains why etch pits are ubiquitous and why protective surface layers of secondary minerals are not observed on the common silicates. The product-reactant volume ratio is greater than one for mineral pairs involving almandine and spessartine garnets and many common weathering products. These volume relationships explain why rate-determining, protective surface layers form on Fe- and Mn-bearing garnets (at least under chemical conditions favoring conservative behavior of Al, Fe, and Mn), and, further, why in the absence of such chemical conditions, protective surface layers cannot form, resulting in interface-limited dissolution and etching. Product-reactant volume ratios, transport properties of the products, and geochemical conditions that determine the solubility of Al, Fe, and Mn explain the distribution of rate-determining mechanisms and the associated etch pits and protective surface layers on naturally weathered silicate minerals.

Acknowledgments

I am grateful to Joe D. McKee for asking the critical question at the right time; Fabrice Colin, Jean Delvigne, Bruno Boulangé, Eduard Bard, Jean-Dominique Meunier, Daniel B. Nahon, Alain Baronnet, Enrique Merino, Duncan F. Sibley, and David T. Long for useful discussions of mineral replacement textures; Alex E. Blum, Robert A. Berner, Susan L. Brantley, Daniel B. Nahon, and Scott Argast for their encouraging and supportive comments; Danita S. Brandt for penetrating and too-often underappreciated editorial comments; Eric J. Essene and Susan L. Brantley for their provocative and thorough reviews of the manuscript; and Robert B. Gordon for introducing me to the Pilling-Bedworth rule and the literature on corrosion. Alan S. Pooley of the Yale Peabody Museum facilitated the scanning electron photomicrography. This paper was written during my sabbatical leave at the Department of Geology, University of Cincinnati, and revised during a visit to the Laboratoire de Géosciences de l'Environnement, Université d'Aix-Marseilles III. I am grateful to my colleagues at both these institutions for their hospitality. Initial research on this project was supported by NSF grants EAR 80-07815 and BSR 85-14328.

References cited

Anand, R.R., and Gilkes, R.J. (1984) Weathering of hornblende, plagioclase and chlorite in meta-dolerite, Australia. Geoderma, 34, 261–280.

Banfield, J.F., and Eggleton, R.A. (1990) Analytical transmission electron microscope studies of plagioclase, muscovite, and K-feldspar weathering. Clays and Clay Minerals, 38, 77–89.

Basham, I.R. (1974) Mineralogical changes associated with deep weathering of gabbro in Aberdeenshire. Clay Minerals, 10, 189–202.

Berner, R.A. (1978) Rate control of mineral dissolution under earth surface conditions. American Journal of Science, 278, 1235–1252.

——— (1981) Kinetics of weathering and diagenesis. Mineralogical Society of America Reviews in Mineralogy, 8, 111–134.

Berner, R.A., and Holdren, G.R. (1977) Mechanism of feldspar weathering: Some observational evidence. Geology, 5, 369–372.

——— (1979) Mechanism of feldspar weathering. II. Observations of feldspars from soils. Geochimica et Cosmochimica Acta, 43, 1173–1186.

Berner, R.A., and Schott, J. (1982) Mechanism of pyroxene and amphi-

bole weathering. II. Observations of soil grains. American Journal of Science, 282, 1214–1231.

Berner, R.A., Sjöberg, E.L., Velbel, M.A., and Krom, M.D. (1980) Dissolution of pyroxenes and amphiboles during weathering. Science, 207, 1205–1206.

Blum, A.E., and Lasaga, A.C. (1987) Monte Carlo simulations of surface reaction rate laws. In W. Stumm, Ed., Aquatic surface chemistry: Chemical processes at the particle-water interface, p. 255–292. Wiley, New York.

Blum, A.E., Yund, R.A., and Lasaga, A.C. (1990) The effect of dislocation density on the dissolution rate of quartz. Geochimica et Cosmochimica Acta, 54, 283–297.

Brantley, S.L., Crane, S.R., Crerar, D.A., Hellman, R., and Stallard, R. (1986) Dissolution at dislocation etch pits in quartz. Geochimica et Cosmochimica Acta, 50, 2349–2361.

Cleaves, E.T. (1974) Petrologic and chemical investigation of chemical weathering in mafic rocks, eastern Piedmont of Maryland. Maryland Geological Survey, Report of Investigations, 25, 28.

Cremeens, D.L., Darmody, R.G., and Jansen, I.J. (1987) SEM analysis of weathered grains: Pretreatment effects. Geology, 15, 401–404.

Delvigne, J. (1983) Micromorphology of the alteration and weathering of pyroxenes in the Koua Bocca ultramafic intrusion, Ivory Coast, West Africa. In D. Nahon and Y. Noack, Eds., Pétrologie des altérations et des sols, volume II, p. 57–68. Sciences Géologiques, Mémoires, Strasbourg, France.

——— (1990) Hypogene and supergene alterations of orthopyroxene in the Koua Bocca ultramafic intrusion, Ivory Coast. Chemical Geology, 84, 49–53.

Delvigne, J., Bisdom, E.B.A., Sleeman, J., and Stoops, G. (1979) Olivines, their pseudomorphs and secondary products. Pedologie, 29, 247–309.

Eggleton, R.A. (1986) The relation between crystal structure and silicate weathering rates. In S.M. Colman and D.P. Dethier, Eds., Rates of chemical weathering of rocks and minerals, p. 21–40. Academic, Orlando, Florida.

Eggleton, R.A., and Buseck, P.R. (1980) High resolution electron microscopy of feldspar weathering. Clays and Clay Minerals, 28, 173–178.

Eggleton, R.A., and Smith, K.L. (1983) Silicate hydration mechanisms. In D. Nahon and Y. Noack, Eds., Pétrologie des altérations et des sols, volume II, p. 45–53. Sciences Géologiques, Mémoires, Strasbourg, France.

Embrechts, J., and Stoops, G. (1982) Microscopical aspects of garnet weathering in a humid tropical environment. Journal of Soil Science, 33, 535–545.

Fromhold, A.T., Jr. (1976) Theory of metal oxidation. I. Fundamentals. Defects in crystalline solids series, volume 9, 547 p. North-Holland, Amsterdam, The Netherlands.

Ghabru, S.K., Mermut, A.R., and St. Arnaud, R.J. (1989) Characterization of garnets in a typic cryoboralf (gray luvisol) from Saskatchewan, Canada. Soil Science Society of America Journal, 53, 575–582.

Glasmann, J.R. (1982) Alteration of andesite in wet, unstable soils of Oregon's western Cascades. Clays and Clay Minerals, 30, 253–263.

Graham, R.C., Weed, S.B., Bowen, L.H., and Buol, S.W. (1989a) Weathering of iron-bearing minerals in soils and saprolite on the North Carolina Blue Ridge Front. I. Sand-size primary minerals. Clays and Clay Minerals, 37, 19–28.

Graham, R.C., Weed, S.B., Bowen, L.H., Amarasiriwardena, D.D., and Buol, S.W. (1989b) Weathering of iron-bearing minerals in soils and saprolite on the North Carolina Blue Ridge Front. II. Clay mineralogy. Clays and Clay Minerals, 37, 29–40.

Grandstaff, D.E. (1978) Changes in surface area and morphology and the mechanism of forsterite dissolution. Geochimica et Cosmochimica Acta, 42, 1899–1901.

Gratz, A.J., Manne, S., and Hansma, P.K. (1991a) Atomic force microscopy of atomic-scale ledges and etch pits formed during dissolution of quartz. Science, 251, 1343–1346.

Gratz, A.J., Bird, P., and Quiro, G.B. (1991b) Dissolution of quartz in aqueous basic solution, 106–236°C: Surface kinetics of "perfect" crystallographic faces. Geochimica et Cosmochimica Acta, 54, 2911–2922.

Hansley, P.L. (1987) Petrologic and experimental evidence for the etching of garnets by organic acids in the upper Jurassic Morrison Formation, northwestern New Mexico. Journal of Sedimentary Petrology, 57, 666–681.

Hauffe, K. (1965) Oxidation of metals, 452 p. Plenum, New York.

Hollabaugh, C.L., Callaham, J.M., Warner, S.J., Kath, R.L., and DeCinque, J.D. (1989) Anatase pseudomorphs after titanite from Fulton County, Georgia and their experimental synthesis. Southeastern Geology, 30, 121–135.

Kubaschewski, O., and Hopkins, B.E. (1962) Oxidation of metals and alloys (2nd edition), 319 p. Butterworths, London.

Lasaga, A.C., and Blum, A.E. (1986) Surface chemistry, etch pits, and mineral-water interactions. Geochimica et Cosmochimica Acta, 50, 2363–2379.

Macaire, J.-J., Perruchot, A., and Dejou, J. (1988) Transformations géochimiques au cours de l'altération météorique d'une basanite Pliocène du Massif Central Français. Geoderma, 41, 287–314.

Maynard, J.B. (1983) Geochemistry of sedimentary ore deposits, 305 p. Springer-Verlag, New York.

Nahon, D.B. (1991) Introduction to the petrology of soils and chemical weathering, 313 p. Wiley, New York.

Nahon, D., and Bocquier, G. (1983) Petrology of elements transfers in weathering and soil systems. In D. Nahon and Y. Noack, Eds., Pétrologie des altérations et des sols, volume II, p. 111–119. Sciences Géologique, Mémoires, Strasbourg, France.

Nahon, D., Colin, F., and Tardy, Y. (1982) Formation and distribution of Mg,Fe,Mn-smectites in the first stages of the lateritic weathering of forsterite and tephroite. Clay Minerals, 17, 339–348.

Nahon, D., Beauvais, A., Nziengui-Mapangou, P., and Ducloux, J. (1984) Chemical weathering of Mn-garnets under lateritic conditions in northwest Ivory Coast (West Africa). Chemical Geology, 45, 53–71.

Nahon, D., Beauvais, A., and Trescases, J.J. (1985) Manganese concentration through chemical weathering of metamorphic rocks under lateritic conditions. In J.I. Drever, Ed., The chemistry of weathering, p. 277–291. Reidel, Dordrecht, The Netherlands.

Parisot, J.C., Delvigne, J., and Groke, M.T.C. (1983) Petrographical aspects of the supergene weathering of garnet in the Serra dos Carajas (Para, Brazil). In D. Nahon and Y. Noack, Eds., Pétrologie des altérations et des sols, volume II, p. 141–148. Sciences Géologique, Mémoires, Strasbourg, France.

Perseil, E.A., and Grandin, G. (1985) Altération supergène des protores à grenats manganésifères dans quelques gisements d'Afrique del'Ouest. Mineralium Deposita, 20, 211–219.

Petrovic, R. (1976) Rate control in feldspar dissolution. II. The protective effect of precipitates. Geochimica et Cosmochimica Acta, 40, 1509–1521.

Salvino, J.F., and Velbel, M.A. (1989) Faceted garnets from sandstones of the Munising Formation (Cambrian), northern Michigan: Petrographic evidence for origin by intrastratal dissolution. Sedimentology, 36, 371–379.

Schott, J., and Berner, R.A. (1983) X-ray photoelectron studies of the mechanism of iron silicate dissolution during weathering. Geochimica et Cosmochimica Acta, 47, 2233–2240.

——— (1985) Dissolution mechanisms of pyroxenes and olivines during weathering. In J.I. Drever, Ed., The chemistry of weathering, p. 35–53. Reidel, Dordrecht, The Netherlands.

Schott, J., and Petit, J.-C. (1987) New evidence for the mechanisms of dissolution of silicate minerals. In W. Stumm, Ed., Aquatic surface chemistry: Chemical processes at the particle-water interface, p. 293–315. Wiley, New York.

Schott, J., Berner, R.A., and Sjöberg, E.L. (1981) Mechanism of pyroxene and amphibole weathering. I. Experimental studies of iron-free minerals. Geochimica et Cosmochimica Acta, 45, 2123–2135.

Schwertmann, U., and Taylor, R.M. (1989) Iron oxides. In J.B. Dixon and S.B. Weed, Eds., Minerals in soil environments (2nd edition), p. 379–438. Soil Science Society of America, Madison, Wisconsin.

Siever, R., and Woodford, N. (1979) Dissolution kinetics and the weathering of mafic minerals. Geochimica et Cosmochimica Acta, 43, 717–724.

Smyth, J.R., and Bish, D.L. (1988) Crystal structures and cation sites of the rock-forming minerals, 332 p. Allen & Unwin, Boston, Massachusetts.

Stoops, G., Altemuller, H.-J., Bisdom, E.B.A., Delvigne, J., Dobrovolsky, V.V., Fitzpatrick, E.A., Paneque, G., and Sleeman, J. (1979) Guidelines for the description of mineral alterations in soil micromorphology. Pedologie, 29, 121–135.

Tazaki, K. (1986) Observation of primitive clay precursors during microcline weathering. Contributions to Mineralogy and Petrology, 92, 86–88.

Tazaki, K., and Fyfe, W.S. (1987a) Primitive clay precursors formed on feldspar. Canadian Journal of Earth Science, 24, 506–527.

——— (1987b) Formation of primitive clay precursors on K-feldspar under extreme leaching conditions. In L.G. Schultz, H. van Olphen, and F.A. Mumpton, Eds., Proceedings of the international clay conference, Denver, 1985, p. 53–58. The Clay Minerals Society, Bloomington, Indiana.

Vance, E.R., and Doern, D.C. (1989) The properties of anatase pseudomorphs after titanite. Canadian Mineralogist, 27, 495–498.

Velbel, M.A. (1983) A dissolution-reprecipitation mechanism for the pseudomorphous replacement of plagioclase feldspars by clay minerals during weathering. In D. Nahon and Y. Noack, Eds., Pétrologie des altérations et des sols, volume I, p. 139–147. Sciences Géologique, Mémoires, Strasbourg, France.

——— (1984a) Natural weathering mechanisms of almandine garnet. Geology, 12, 631–634.

——— (1984b) Weathering processes of rock-forming minerals. In M.E. Fleet, Ed., Environmental geochemistry, p. 67–111. Mineralogical Association of Canada Short Course Handbook 10, Toronto, Ontario.

——— (1986) Influence of surface area, surface characteristics, and solution composition on feldspar weathering rates. In J.A. Davis and K.F. Hayes, Eds., Geochemical processes at mineral surfaces, p. 615–634. American Chemical Society, Symposium Series, no. 323, Washington, DC.

——— (1987) Rate-controlling factors in the weathering of some ferromagnesian silicate minerals. Transactions, 13th Congress of the International Society of Soil Science, Hamburg, Germany, 6, 1107–1118.

——— (1989) Weathering of hornblende to ferruginous products by a dissolution-reprecipitation mechanism: Petrography and stoichiometry. Clays and Clay Minerals, 37, 515–524.

White, A.F., and Yee, A. (1985) Aqueous oxidation-reduction kinetics associated with coupled electron-cation transfer from iron-containing silicates at 25°C. Geochimica et Cosmochimica Acta, 49, 1263–1275.

White, A.F., Yee, A., and Flexser, S. (1985) Surface oxidation-reduction kinetics associated with experimental basalt-water reaction at 25°C. Chemical Geology, 49, 73–86.

Wilson, M.J. (1975) Chemical weathering of some primary rock-forming minerals. Soil Science, 119, 349–355.

Manuscript received May 9, 1991
Manuscript accepted November 20, 1992